J Ther Eng, Vol. 10, No. 6, pp. 1423−1439, November, 2024

Journal of Thermal Engineering
Web page info: https://jten.yildiz.edu.tr
DOI: 10.14744/thermal.0000884

Research Article

Exergetic performance evaluation of a phase change material integrated solar still

Sudeepthi A.[1], **Arun P.**[2,*]

[1]Wolfson Department of Chemical Engineering, Technion-Israel Institute of Technology, Haifa, 3200003, Israel
[2]Department of Mechanical Engineering, National Institute of Technology Calicut, 673601, India

ARTICLE INFO

Article history
Received: 28 February 2023
Revised: 10 January 2024
Accepted: 11 January 2024

Keywords:
Double Slope Solar Still; Energy Storage; Exergy Efficiency; Phase Change Material (PCM); Thermal Efficiency; Volumetric Heat Generation

ABSTRACT

Solar desalination has a significant potential for addressing the increasing water scarcity of the world. Solar stills offer a sustainable solution for desalination of brackish water. Integration of Phase Change Material (PCM) in the still is one of the options for enhancing its productivity. Integration of PCM in solar stills has gained attention due to its capability to efficiently store and release thermal energy thereby enhancing its productivity. The present work proposes a modeling framework for the performance assessment of simple double slope solar stills integrated with PCM. The methodology is based on energy and exergy balance of the overall system. The exergy destruction associated with the still has been evaluated for the basic still and is compared with the case of PCM integrated still. The developed mathematical modeling framework is validated based on comparisons with the experimental observations for the south Indian location of Kozhikode. Lauric acid is considered as the representative PCM due to its favorable thermal properties for the application in solar stills. There is a reasonable agreement between the theoretical and experimental observations. With the incorporation of lauric acid as the PCM in the system, daily yield, daily thermal efficiency and exergy efficiency were found to be increased by 8.9%, 10.6%, and 3% respectively. A generic modelling framework for energy and exergy-based performance assessment of a PCM integrated still has been presented, which will be a useful tool for system optimization. Integration of different PCM with enhanced thermal properties are planned as future work for overall system optimisation for maximum energy efficiency.

Cite this article as: A. S, P. A. Exergetic performance evaluation of a phase change material integrated solar still. J Ther Eng 2024;10(6):1423−1439.

INTRODUCTION

Clean potable water is a basic necessity for humankind. Population expansion, industrialization, and ground water extraction have all led to a significant increase in the need for potable water [1]. The uninterrupted availability of clean water is a major global issue, especially for developing countries. Desalination of brackish water/briny water offers one possible solution for meeting the shortage of clean water. The ever-growing demand can be met effectively by

***Corresponding author.**
*E-mail address: arun.p@nitc.ac.in

This paper was recommended for publication in revised form by Editor-in-Chief Ahmet Selim Dalkılıç

Published by Yıldız Technical University Press, İstanbul, Turkey

desalination utilizing a solar still, which is an affordable technology [2]. Solar desalination is a promising option to overcome the problem of potable water scarcity. Though solar stills offer a sustainable alternative to conventional desalination systems, they suffer from low productivity. Improvement of solar desalination systems is an active area of research. A review of the various types of solar stills has been reported by Malaiyappan and Elumalai [3]. Thakur et al. [4] in their recent study observed that the maximum productivity of active solar still was 10 litres per day and in passive solar stills, it was 6 litres per day. Gaur et al. [5] studied the effect of flowing water over the glass cover of a active solar still and reported increase in thermal efficiency and daily exergy output by 4% and 8.2% respectively, for this improved system over the conventional type. Many methods have been proposed to improve the productivity of solar stills [6, 7]. Rani et al. [8] investigated the performance of single slope solar still coupled with a flat plate solar collector and reported that the overall efficiency reached up to 9.86% in natural mode and 16.70% in forced mode. Al-Qasaab et al. [9] reported the design and fabrication of a parabolic dish integrated with innovative single slope solar still to distil saltwater and studied the winter productivity for the climatic conditions of Najaf in Iraq. A study conducted by Javadi Yanbolagh et al. [10] for Tehran revealed that a distillation system with thermoelectric heating modules exhibited most favorable exergo-economic and enviro-economic performance and acceptable energy payback time (EPBT). Incorporation of energy storage within the system has been found to be a promising option in this regard. Sensible as well as latent heat storage systems have been used in solar stills. Quartzite rock, red brick, washed stones and iron scraps have been used as sensible energy storage materials in solar stills [11]. The effect of using different sensible heat storage materials on a single slope solar still provided with a dripping saline water arrangement and calcium stone as energy storage showed an increase of 36% in productivity [12]. Desalination could be improved by employing phase-change materials (PCM) [13]. Latent heat storage using PCMs find wide applications ranging from spacecraft to solar thermal systems, including stills [14]. The dissipated heat is stored in PCM and used for desalination during the evening and night to boost the production of a solar still [2]. A comparison of solar still using internal reflector and composite black gravel phase changing material for thermal heat storage were carried out. Two different modes were considered: one with composite material and the other with PCM [15]. Using single organic PCM would not be adequate to get the desired productivity or performance in different environmental conditions for a solar still. Incorporating multiple organic PCMs to create binary eutectic PCM would increase the thermophysical properties. The energy efficiency is found to be increased using this modified PCM integrated solar stills [1]. Many experiments were conducted using different fatty acids as PCM to enhance the solar still performance in terms of productivity. The experiments with three different fatty acids with pin fins were incorporated for better heat transfer. The conventional solar still energy, exergy and economic analysis were compared with those with different fatty acid with pin fins. It was found that the productivity, exergy and energy efficiencies were more for the solar still using fatty acid as PCMs [16]. The distillates produced using three different PCMs namely lauric acid, stearic acid paraffin wax stored in copper cylinder were compared. Here cylindrical storage of PCMs have rendered better performance than spherical storage. Lauric acid performed well compared to other two when stored in copper cylinders [17]. Most of the PCM faced the issue of having low thermal conductivity and discharge energy. The developed shape stabilized PCM shows high thermal conductivity to overcome the difficulty faced by conventional PCMs [18]. The analysis and multi-objective optimization (MOO) of weir-type solar still systems using phase change material (PCM) with regard to the energetic and financial performance were examined [19]. Khandagre et al. [20] reported an efficiency improvement by 42% with magnesium sulphate heptahydrate as the PCM in a double slope solar still for the climatic conditions of Jabalpur, India. Many works were performed for thorough analysis of modern modelling techniques in solar stills. Different thermal models were proposed and derived for various types of solar stills, and the alterations were suggested to improve performance [21]. Transient mathematical models to evaluate the performance of solar still with and without PCM as thermal energy storage media had been investigated [22]. It was studied how well a cascade solar still worked with PCM storage, and it was found that the still with PCM displayed 31% higher productivity than the still without PCM [23]. Analysis of a passive solar still used for desalination of brackish water with PCM integrated below the liner was carried out using mathematical modeling for Errachidia city, Morocco. It was observed that the choice of the PCM is linked to the maximum temperature attained by the brackish water in the basin [24]. For various types of stills, several studies had been carried out to evaluate the performance of the stills based on energy and exergy analyses. The analysis is typically based on energy and exergy balance accounting for the mass and energy transfers associated with the various components of the system. Exergy analysis of a shallow solar still revealed that irreversibility rates in brine and glass cover were negligible while exergy destruction was highest for the collector. For the same exergy input to the collector, brine and solar still exergy efficiencies of 12.9%, 6%, and 5% were reported [25]. The exergy analysis of a PCM incorporated passive solar still was illustrated for a location in Morocco, to compute the exergy destruction during the phase change process. Paraffin wax was used as the PCM and variations of PCM temperature, exergy destruction within the still and that of PCM medium, still productivity and exergy efficiency had been analyzed. It was observed that latent heat storage improved the still productivity while there was a drop in the exergy efficiency [26]. Effect of the presence of a condenser and the medium of saline water types on the performance of the solar still has been investigated. It was observed that using a glass condenser and by placing black steel fibers inside the water basin increased the daily productivity of the still by 35% [27]. Annual performance of single basin single slope, double slope, and pyramidal shaped solar stills were studied experimentally and theoretically for the climatic conditions of Jordan. It was concluded from this study that optimal system could be a south oriented single slope solar still with a tilt angle of about 30°, water depth of about 1 cm, and insulation thickness of about 4 cm [28]. Performance analysis of modified basin type double slope multi-wick solar still for Allahabad, India had been reported. The overall thermal efficiency of the system with jute and black cotton wicks were found to be 21% and 23%, respectively [29]. A comparative study of energy and exergy performance of two weir type cascade solar stills, with and without PCM storage, in clear and partially cloudy days had been carried out. The study indicated that energy and exergy performance of solar still without PCM storage was found to be better than the solar still with PCM storage on clear days. The solar still with PCM storage was found to be better for partly-cloudy days due to its better energy and exergy efficiencies. The maximum energy and exergy efficiencies of the solar still with PCM for a typical partly-cloudy day were observed to be 74% and 8.5% respectively [30]. Based on a review of several types of solar stills, it has been observed that energy efficiency of conventional solar stills lies in the range of 20-46% and the still productivity is mostly less than 6 litres/m^2/day. The exergetic efficiency for single effect systems which are widely used is often less than 5% [31]. It has been observed that only limited studies have investigated the effect of incorporating energy storage using PCM like lauric acid on the exergy efficiency of the stills. The computation of irreversibility associated with different components of the still will help in optimizing the system performance.

PCM INTEGRATED SOLAR STILL

A typical solar still works on evaporation-condensation cycle driven by the incident solar radiation. The present work investigates the performance of a modified basin-type solar still integrated with PCM. Schematic diagrams of basic double slope passive solar still and the modified one with the incorporation of PCM are shown in Figure 1. During sunshine hours, thermal energy is stored in the PCM as it changes phase from solid to liquid. During the no-sunshine periods, temperatures of all the components of the still drop, but the PCM temperature remains higher than that of ambient. PCM starts discharging the heat stored in it to the brackish water by the liquid to solid phase change. Therefore, the evaporation of brackish water takes place even during periods of no-sunshine. Among the available material for use as PCM, organic PCMs have been a preferred choice due to their favorable properties as compared to inorganic and eutectic ones. Organic PCMs are further classified into paraffins and non-paraffins (fatty acids). Fatty acids have a high heat of fusion (comparable to widely used paraffins), are only mildly corrosive and also show reproducible melting and freezing behavior and freeze with no super-cooling [14]. Taking these factors into consideration along with suitability of the melting temperature (40-45°C), a non-paraffin compound, lauric acid ($CH_3(CH_2)_{10}.COOH$) has been chosen for the present work [9]. The current cost (about 17 USD/kg), long shelf life and non-toxicity have also been considered for the PCM selection. A laboratory scale experimental unit with basic instrumentation was set up for the investigations on still incorporating PCM at Solar Energy Centre of National Institute of Technology Calicut.

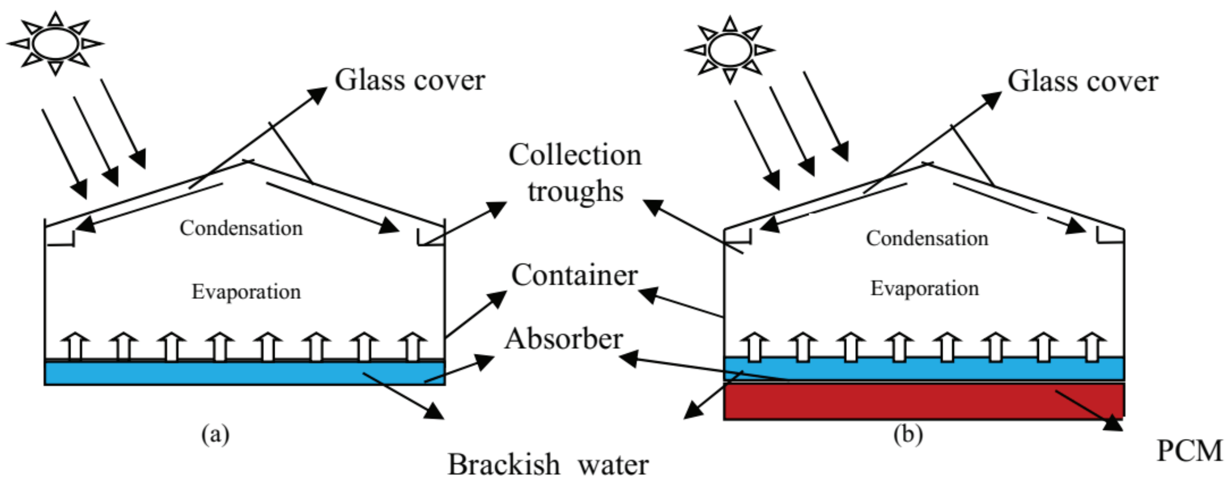

Figure 1. Schematic of (a) basic double slope solar still (b) still with the integration of PCM.

Basin of the still was made up of 0.0015 m thick galvanized iron sheet of dimensions: 0.60 m x 0.30 m x 0.15 m. The inner surface was coated with black paint to form the absorber section. Two glass covers of 0.31 m x 0.30 m were mounted on the basin top. Inlet and outlet holes of 12 mm diameter were provided on the side wall and basin bottom. Outlet holes for distilled water were provided at the two ends along the length of the still. A 20-litre tank was used to supply brackish water feed. Sides and bottom of the basin were well insulated using expandable styrofoam to reduce the heat losses to the surroundings. Sealants were used for preventing water leakage and rubber gaskets were provided for avoiding vapour leak. To incorporate PCM, a container arrangement was fabricated to store the PCM ensuring uniform contact with the basin liner. PCM is stored in the trays which are integral to the container. The whole arrangement was provided as an add-on module to the basic still ensuring contact with the bottom of the still which houses the basin liner. The container and tray arrangement proposed in this work gives the flexibility to perform tests with different masses of PCM. The schematic diagrams of the still and the container-tray arrangement (with dimensions) are given in Figure 2. The specifications of the still are given in Table 1. Experiments were conducted in NIT Calicut with and without PCM in the alternate weeks of March. Glass temperature, water temperature, absorber temperature, yield (amount of potable water output), global solar radiation, wind speed are measured at the end of each hour from 9 AM to 9 PM without PCM. During the experimentation with PCM, PCM temperature was also measured along with the above-mentioned parameters. During the experimentation brackish water level in the basin was maintained at constant height of 1 cm. Brackish

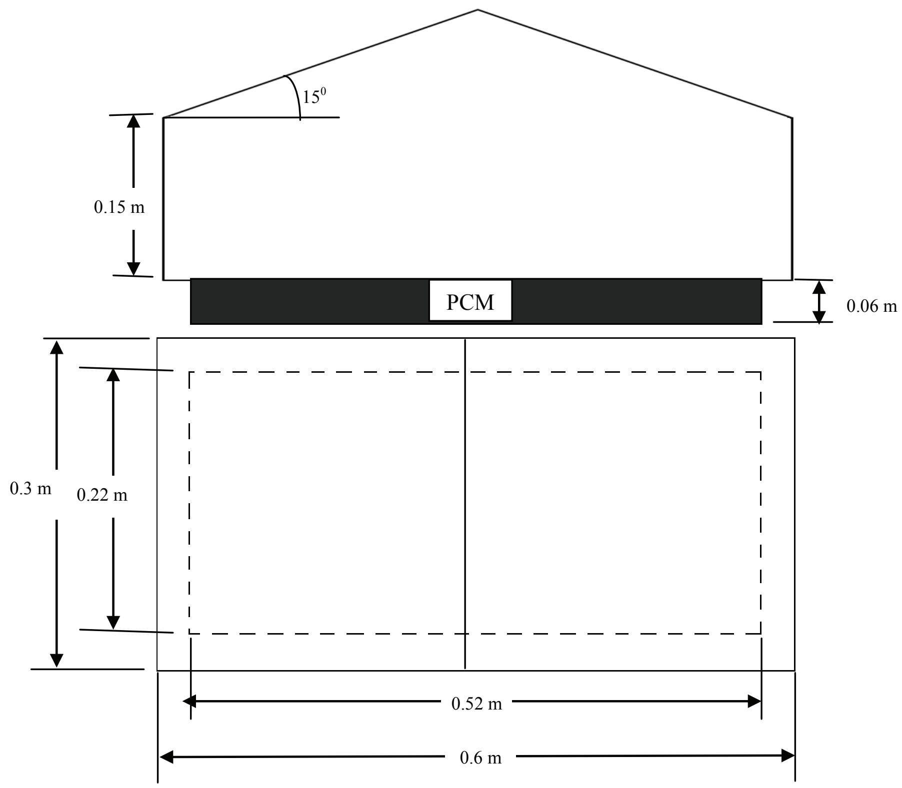

(a)

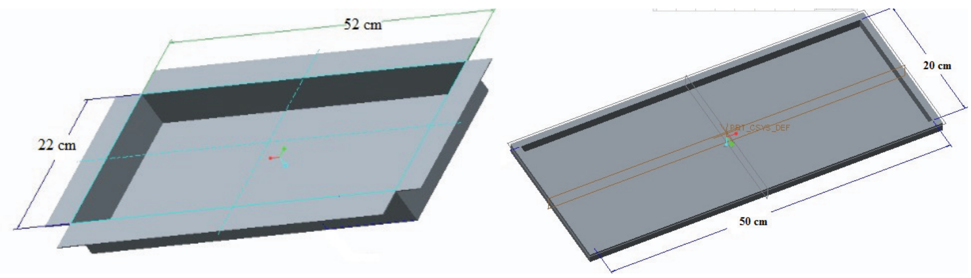

(b)

Figure 2. (a) Schematic diagram of the still (b) container and tray arrangement for the PCM storage.

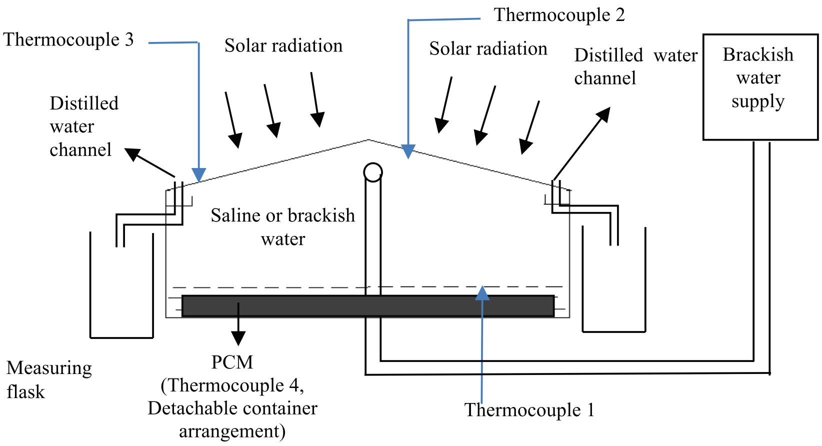

(a)

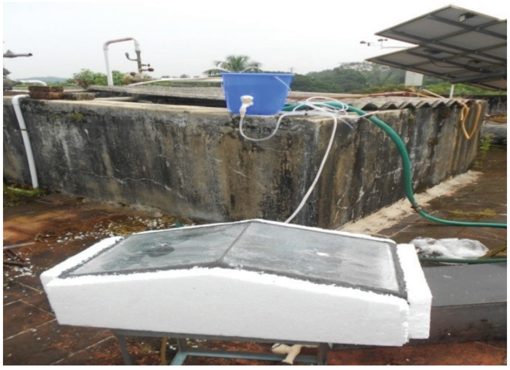

(b)

Figure 3. (a) Layout of the experimental setup. (b) Photograph of the experimental setup.

water container was kept sufficiently above the still level to ensure water supply by gravity feed. Water flow to the still was controlled by a valve fixed to the container. Water can be drained from the still through the outlet provided at the bottom. The significant parameters observed at hourly intervals during the experiments were: (1) glass cover temperature (2) basin water temperature (3) absorber temperature (4) PCM temperature (5) yield (6) global solar radiation (7) wind speed (8) atmospheric pressure. Calibrated T type thermocouples were attached to the glass cover, water, absorber and PCM to measure the temperatures. Effect of irradiance on the thermocouple has not been explicitly considered in the study. Global solar radiation, wind speed, ambient temperature and atmospheric pressure were measured using a standard weather station. Measuring flasks were used to measure the yield from the still. The layout of the experimental setup is shown in Figure 3.

Table 1. Specifications of the still

Type	Double slope
Area of glass cover	0.186 m^2
Glass type	Float glass
Glass cover inclination	15°
Area of basin	0.18 m^2
Length of the basin	0.6 m
Breadth of the basin	0.3 m
Material for basin and collection troughs	Galvanized iron
Insulation material	Expandable Polystyrene
Thickness of insulation	0.03 m

System Modelling and Simulation

Mathematical model formulated for performance assessment of the PCM integrated still is described in this section. Model equations reported in the literature have been suitably modified for the simulation of the experimental system. The system model, correctly validated with the experimental results helps in the performance assessment of the system under varied climatic conditions and aids in optimizing the system. Comparison of the basic still and still with the integration of PCM is carried out using both energy and exergy analyses.

Energy Analysis of the System

Energy balance for various components of the still is considered to obtain the major system parameters. The following assumptions are made while obtaining the energy balance equations:

(i) There is no vapor leakage to the surroundings.
(ii) There are no temperature gradients across glass, absorber and along saline water depth.
(iii) Side losses of the still and reflectivity of the saline water have been neglected.

For the basic still, energy balance for glass cover is given by [32]:

$$\frac{m_g c_g}{A_g}\frac{dT_g}{dt} = (1-\rho_g)\alpha_g I + (q_{r,w-g} + q_{c,w-g} + q_{e,w-g}) - (q_{c,g-a} + q_{r,g-a}) \tag{1}$$

The heat transfer from the glass cover to atmosphere comprises of convection and radiation modes. They are expressed respectively as follows [32]:

$$q_{c,g-a} = h_{c,g-a}(T_g - T_a) \tag{2}$$

$$q_{r,g-a} = h_{r,g-a}(T_g - T_a) \tag{3}$$

The convective and radiative heat transfer coefficients from glass cover to the atmosphere are calculated based on the following expressions [33, 34]:

$$h_{c,g-a} = 2.8 + 3V \text{ (V≤5m/s) else } 6.15V^{0.8} \text{ (V> 5m/s)} \tag{4}$$

$$h_{r,g-a} = 0.9\,\sigma \frac{T_g^4 - T_{sky}^4}{T_g - T_a} \tag{5}$$

$$\text{where, } T_{sky} = T_a - 6 \tag{6}$$

Energy balance for water in the still is given by [32]:

$$\frac{m_w c_w}{A_w}\frac{dT_w}{dt} = (1-\rho_g)(1-\alpha_g)\alpha_w I + q_{b-w} - (q_{r,w-g} + q_{c,w-g} + q_{e,w-g}) \tag{7}$$

The heat transfer between water and glass cover comprises of radiation, convection and evaporation. Equations for determining the corresponding heat transfer rates are given by:

$$q_{r,w-g} = h_{r,w-g}(T_w - T_g) \tag{8}$$

$$q_{c,w-g} = h_{c,w-g}(T_w - T_g) \tag{9}$$

$$q_{e,w-g} = h_{e,w-g}(T_w - T_g) \tag{10}$$

The radiative, convective and evaporative heat transfer coefficients from still water to glass cover are given by the following expressions [9, 10]:

$$h_{r,w-g} = \varepsilon\,\sigma\left[T_w^2 + T_g^2\right](T_w - T_g) \tag{11}$$

where,

$$\varepsilon = \left[\frac{1}{\varepsilon_w} + \frac{1}{\varepsilon_g} - 1\right]^{-1} \tag{12}$$

$$h_{c,w-g} = 0.884\left[(T_w - T_g) + \frac{(P_w - P_g)(T_w)}{268900 - P_w}\right]^{1/3} \tag{13}$$

$$\text{where, } P(T) = \exp\left(25.317 - \frac{5144}{T}\right) \tag{14}$$

$$h_{e,w-g} = 0.016273 h_{c,w-g}\frac{(P_w - P_g)}{(T_w - T_g)} \tag{15}$$

Energy balance for absorber is given by:

$$\frac{m_b c_b}{A_b}\frac{dT_b}{dt} = (1-\rho_g)(1-\alpha_g)(1-\alpha_w)\alpha_b I - q_{b-w} - q_{loss} \tag{16}$$

The rate of heat transfer between absorber to water is given by:

$$q_{b-w} = h_{b-w}(T_b - T_w) \tag{17}$$

Heat transfer coefficient associated with the heat transfer between absorber and water is given by [35]:

$$h_{b-w} = \frac{Nu k_w}{L_w} \tag{18}$$

$$\text{Where, } Nu = 0.54 Ra^{0.25} \text{ if } 10000 \le Ra \le 8\times10^6$$
$$= 0.15 Ra^{0.33} \text{ if } Ra > 8\times10^6$$

Here Ra is a dimensionless parameter that characterizes the onset of natural convection and heat transfer within the system.

Heat loss to the surroundings from the absorber is expressed as:

$$q_{loss} = U_{b-a}(T_b - T_a) \tag{19}$$

Where, U_{b-a} is overall heat transfer coefficient associated with the heat losses to the ambient from the absorber, given by the following expression:

$$U_b = \left[\frac{L_b}{k_b} + \frac{L_i}{k_i} + \frac{1}{h_i}\right]^{-1} \tag{20}$$

For the still integrated with PCM, equations (1) to (15) remain the same while the energy balance for absorber and PCM are modified as given below:

Energy balance for absorber:

$$\frac{m_b c_b}{A_b}\frac{dT_b}{dt} = (1-\rho_g)(1-\alpha_g)(1-\alpha_w)\alpha_b I - q_{b-w} - q_{b-pcm} \tag{21}$$

An expression for the heat transfer rate between the absorber and PCM is given by [20]:

$$q_{b-pcm} = \frac{k_{pcm}}{L_{pcm}}\left(T_b - T_{pcm}\right) \tag{22}$$

Energy balance for PCM:

$$\frac{C_{eq}}{A_{pcm}}\frac{dT_{pcm}}{dt} = q_{b-pcm} - q_{pcm-a} \tag{23}$$

where, the equivalent heat capacity of the used PCM is estimated by [9]:

$$\begin{aligned} C_{eq} &= m_{pcm} c_{s,pcm} && \text{if } T_{pcm} < T_m \\ C_{eq} &= \frac{(m_{pcm} L_{pcm})}{\delta T} && \text{if } T_m \le T_{pcm} \le T_m + \delta T \\ C_{eq} &= m_{pcm} c_{l,pcm} && \text{if } T_{pcm} > T_m + \delta T \end{aligned} \tag{24}$$

Heat loss to the surroundings from the PCM is computed as:

$$q_{pcm-a} = U_{pcm}\left(T_{pcm} - T_a\right) \tag{25}$$

where,

$$U_{pcm} = \left[\frac{L_{pcm}}{k_{pcm}} + \frac{L_i}{k_i} + \frac{1}{h_i}\right]^{-1} \tag{26}$$

The yield and thermal efficiency of the still are obtained as [11]:

$$\text{Hourly yield per unit area} = \frac{q_{e,w-g}}{LH} \times 3600 \tag{27}$$

$$\text{Daily yield per unit area (M)} = \sum_{H=1}^{24}\left[\frac{q_{e,w-g}}{LH}\right] \times 3600 \tag{28}$$

$$\text{Overall thermal efficiency} = \frac{M \times LH}{3600 \times \sum_{H=1}^{24} I} \times 100\% \tag{29}$$

Exergy Analysis of the System

Exergy balance equations are written for the various components of the still to find the irreversibility in each component and hence to find the overall exergy efficiency of the still. These equations are as follows [36, 37]:

From exergy balance for the glass cover:

$$Ex_{d,g} = \alpha_g Ex_{sun} + \left(Ex_{r,w-g} + Ex_{c,w-g} + Ex_{e,w-g}\right) - Ex_{g-a} \tag{30}$$

where, $Ex_{d,g}$ is the exergy destroyed in the glass cover.

Exergy associated with the heat transfer from glass to the atmosphere and the exergy of solar radiation are expressed respectively as follows:

$$Ex_{g-a} = \left(h_{c,g-a} + h_{r,g-a}\right)\left(T_g - T_a\right)\left[1 - \frac{T_a}{T_g}\right] \tag{31}$$

$$Ex_{sun} = I\left[1 + \frac{1}{3}\left(\frac{T_a}{T_S}\right)^4 - \frac{4}{3}\frac{T_a}{T_S}\right] \tag{32}$$

From exergy balance for water:

$$Ex_{d,w} = \tau_g \alpha_w Ex_{sun} + Ex_{b-w} - \left(Ex_{r,w-g} + Ex_{c,w-g} + Ex_{e,w-g}\right) \tag{33}$$

where, $Ex_{d,w}$ is the exergy destroyed in the water.

Exergy associated with the heat transfer from water to glass is the sum of the exergies associated with radiative, convective and evaporative heat transfer and they are computed by the expressions given below:

$$Ex_{r,w-g} = h_{r,w-g}\left(T_w - T_g\right)\left[1 + \frac{1}{3}\left(\frac{T_a}{T_w}\right)^4 - \frac{4}{3}\frac{T_a}{T_w}\right] \tag{34}$$

$$Ex_{c,w-g} = h_{c,w-g}\left(T_w - T_g\right)\left[1 - \frac{T_a}{T_w}\right] \tag{35}$$

$$Ex_{e,w-g} = h_{e,w-g}\left(T_w - T_g\right)\left[1 - \frac{T_a}{T_w}\right] \tag{36}$$

Exergy associated with the heat transfer from the absorber to water is expressed as:

$$Ex_{b-w} = h_{b-w}\left(T_b - T_w\right)\left[1 - \frac{T_a}{T_b}\right] \tag{37}$$

From exergy balance for absorber:

$$Ex_{d,b} = \tau_g \tau_w \alpha_b Ex_{sun} - \left(Ex_{b-w} + Ex_{b-a}\right), \text{ without PCM} \tag{38a}$$

$$Ex_{d,b} = \tau_g \tau_w \alpha_b Ex_{sun} - \left(Ex_{b-w} + Ex_{b-pcm}\right), \text{ with PCM} \tag{38b}$$

where, $Ex_{d,b}$ is the exergy destroyed in the absorber.

Exergy associated with the heat transfer from the absorber to the atmosphere is given by:

$$Ex_{b-a} = U_b\left(T_b - T_a\right)\left[1 - \frac{T_a}{T_b}\right] \tag{39}$$

Overall exergy efficiency, $$Ex_{eff} = \frac{\sum_{H=1}^{24} Ex_{out}}{\sum_{H=1}^{24} Ex_{in}} \times 100\% \tag{40}$$

where, $$Ex_{in} = I\left[1 + \frac{1}{3}\left(\frac{T_a}{T_S}\right)^4 - \frac{4}{3}\frac{T_a}{T_S}\right] \tag{41}$$

$$Ex_{out} = h_{e,w-g}\left(T_w - T_g\right)\left[1 - \frac{T_a}{T_w}\right] \tag{42}$$

System Simulation

The set of differential equations governing the temperature variation of the glass cover, water, absorber and PCM are solved simultaneously using fourth order Runge-Kutta method. The fourth-order Runge-Kutta method is a numerical technique used to approximate the solutions of ordinary differential equations (ODEs). It involves four stages or steps to compute the next approximation of the solution at a particular point. In each stage, it calculates weighted averages of function evaluations at different points within the current interval. These weighted averages are then used to update the solution, resulting in a more accurate approximation compared to simpler methods like Euler's method. A computer program has been developed in C language to simulate the system by the solutions of energy balance equations developed for the different components of the still. At the start of the simulation, the initial temperatures of all the components of the still are assumed to at ambient temperature. Based on the assumed initial temperature values and known physical properties, the heat transfer coefficients are calculated and they are used to estimate the temperatures for the subsequent time step. Following the sequential simulation-based approach, variations of glass temperature, water temperature, absorber temperature and PCM temperature are obtained. The various parameters used for the system simulation are given in Table 2. Thermo-physical properties of the PCM considered in the analysis are given in Table 3.

Table 2. Parameters used for the system simulation [30, 35]

Parameter	Symbol	Value	Unit
Mass of glass cover	m_g	1.4	kg
Specific heat of glass	C_g	800	J/kg K
Absorptivity of glass cover	α_g	0.05	-
Reflectivity of glass cover	ρ_g	0.0745	-
Area of glass cover	A_g	0.186	m^2
Mass of water	m_w	2	kg
Absorptivity of water	α_w	0.05	-
Water depth	L_w	0.01	m
Mass of absorber	m_b	2.5	kg
Specific heat of absorber	C_b	500	J/kgK
Absorptivity of absorber	α_b	0.7	-
Area of absorber	A_b	0.18	m^2
Thickness of absorber	L_b	0.0015	m
Thermal conductivity of absorber	k_b	61	W/mK
Thickness of insulation	L_i	0.03	m
Thermal conductivity of insulation	k_i	0.035	W/mK

Table 3. Thermo-physical properties of the PCM [17]

Phase Change Material	Lauric acid
Melting temperature	43-45 °C
Latent heat	178 kJ/kg
Solid density	880 kg/m^3
Liquid density	760 kg/m^3
Thermal conductivity (solid)	0.442 W/mK
Thermal conductivity (liquid)	0.147 W/mK

RESULTS AND DISCUSSION

The developed mathematical model is validated based on a comparison of the results obtained using system simulation with the experimental observations. The experimental observations were obtained using the laboratory scale still described in earlier section. Experimental data are based on the operation of the still under clear sky conditions in March when a good amount of solar insolation is available in Kozhikode.

Model Validation

The variations of brackish water temperature and glass temperature for a typical day in March for Kozhikode compared with the simulated results are shown in Figures 4 and 5 for the basic still. RMS errors of 18.5% and 8% are obtained for the predictions of the water temperature and glass temperature respectively. The variations of brackish water temperature and glass temperature for a typical day compared with the simulated results are shown in Figures 6 and 7 for the PCM integrated still. RMS errors of 19% and 15.2% are obtained for the predictions of the water temperature and glass temperature respectively for the PCM integrated still. Comparisons of the theoretical and experimental values of daily yield are represented in Figure 8 for the basic still and the PCM integrated still. For the basic still (without PCM), experimental and theoretical daily yields are 1722 ml/m^2 and 1988 ml/m^2 respectively. For the PCM integrated still, experimental and theoretical daily yields are 1944 ml/m^2 and 2165 ml/m^2 respectively. It is observed that there is a reasonable agreement between the theoretical predictions and the experimental observations, though several simplifying assumptions were made in the modelling.

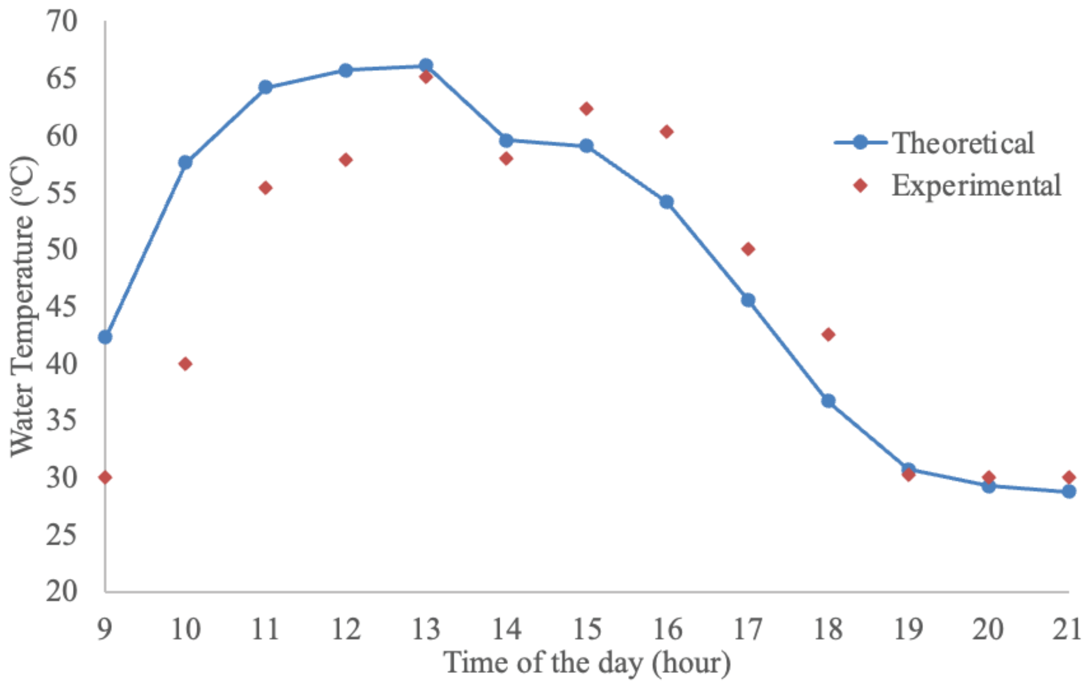

Figure 4. Variation of brackish water temperature for the basic still.

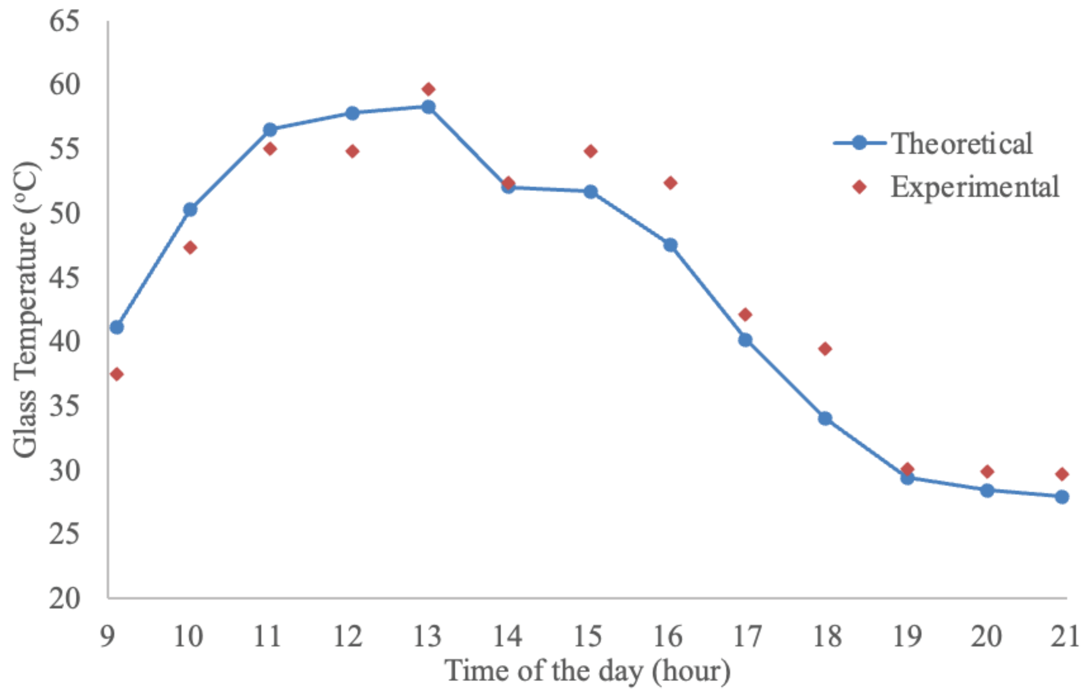

Figure 5. Variation of glass temperature for the basic still.

J Ther Eng, Vol. 10, No. 6, pp. 1423−1439, November, 2024

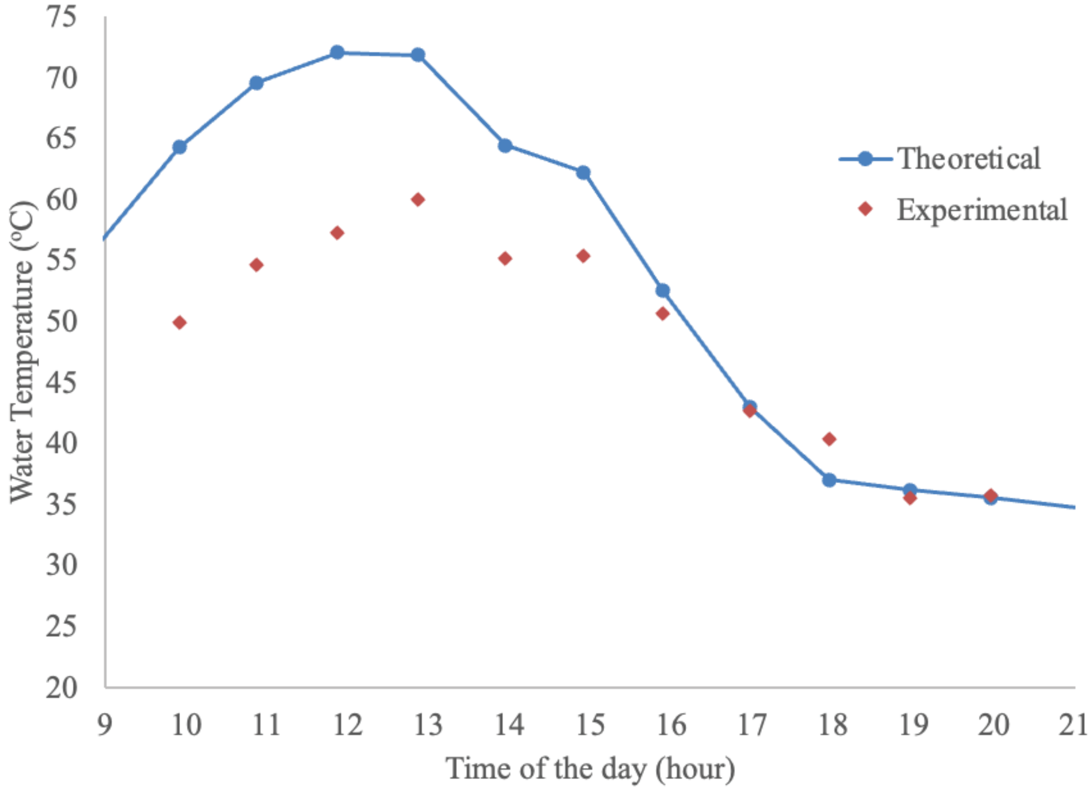

Figure 6. Variation of brackish water temperature for the PCM integrated still.

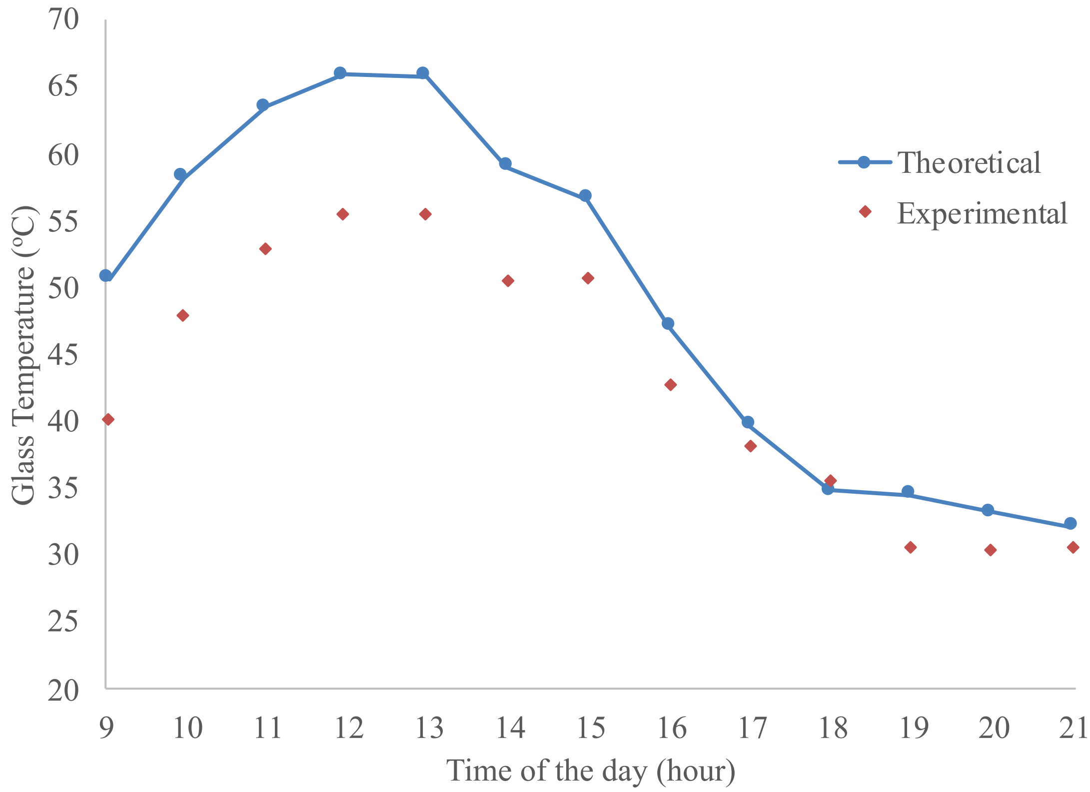

Figure 7. Variation of glass temperature for the PCM integrated still.

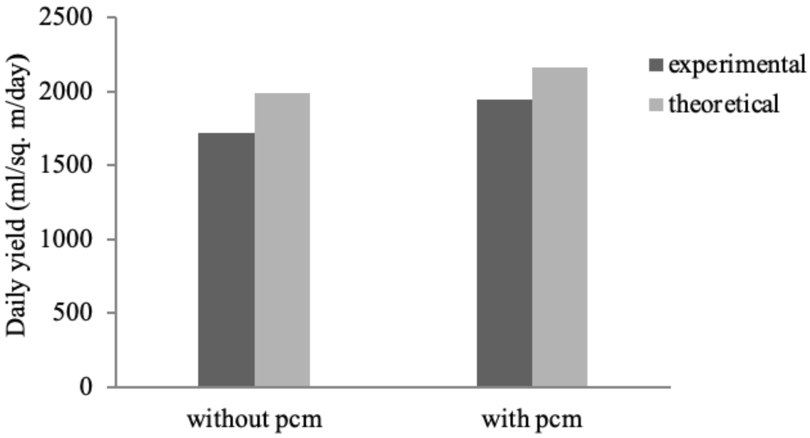

Figure 8. Comparison of yields of the basic still and PCM integrated still.

System Simulation-based Performance Analysis

Figures 9 and 10 illustrate the hourly variation in the temperatures of the components of the still for the basic still and the PCM integrated still respectively. From these figures, it is observed that the temperatures of absorber and water are slightly lower for the PCM integrated still as compared to the basic still. For the basic still, during night time, the temperatures of still components become equal to the ambient temperature. For the still integrated with PCM, PCM will be at an elevated temperature, compared to the components of the still even during the night. Hence PCM discharges the heat stored in it to the brackish water thereby increasing the water temperature.

This result in water temperature being higher than the glass temperature during night periods for the still integrated with PCM, as observed in Figure 10.

The daily yields of the still with and without PCM are 2165 ml/m^2 and 1988 ml/m^2 respectively. The daily yield of the still is improved by 8.9% with the incorporation of PCM. From Figure 11 it is observed that the hourly yield is always higher for the still with PCM. The evaporative heat transfer coefficient from water to glass is always higher for the still with PCM as compared to the basic still as observed from Figure 12.

Evaporative heat transfer coefficient is found to decrease rapidly after 7 PM for the still without PCM, and it is almost zero from 8 PM. Hence there is no yield during night for the still without PCM. In the PCM integrated still, though evaporative heat transfer coefficient continued to decrease after 7 PM, the decrease is not as rapid as that of the still without PCM and its value has not become zero till 2 AM. The daily thermal efficiency

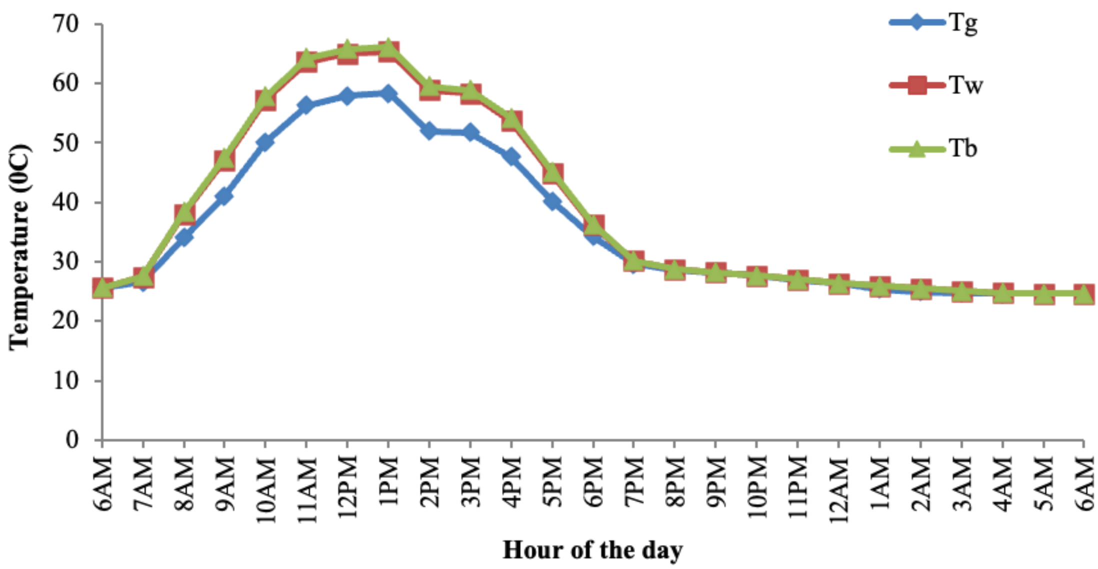

Figure 9. Variation of the temperatures of the still components (basic still).

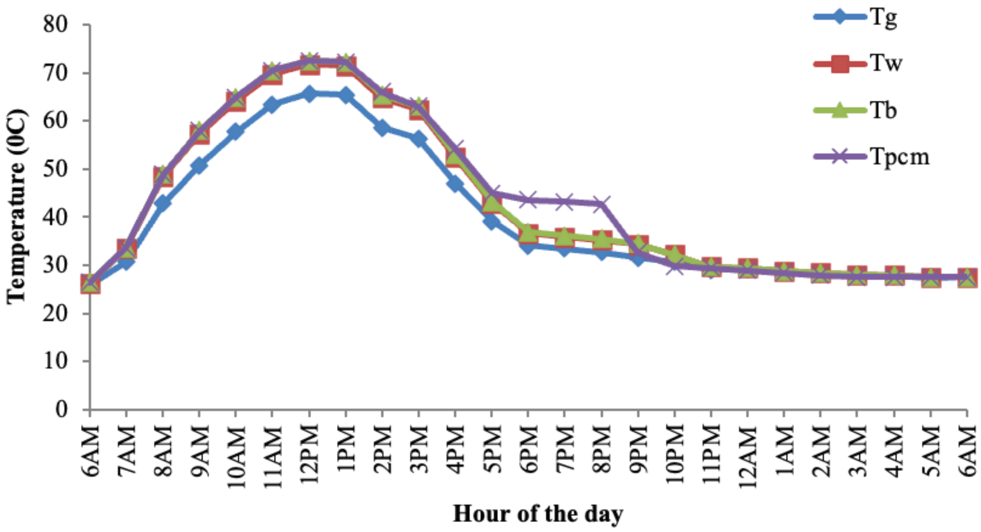

Figure 10. Variation of the temperatures of the still components (PCM integrated still).

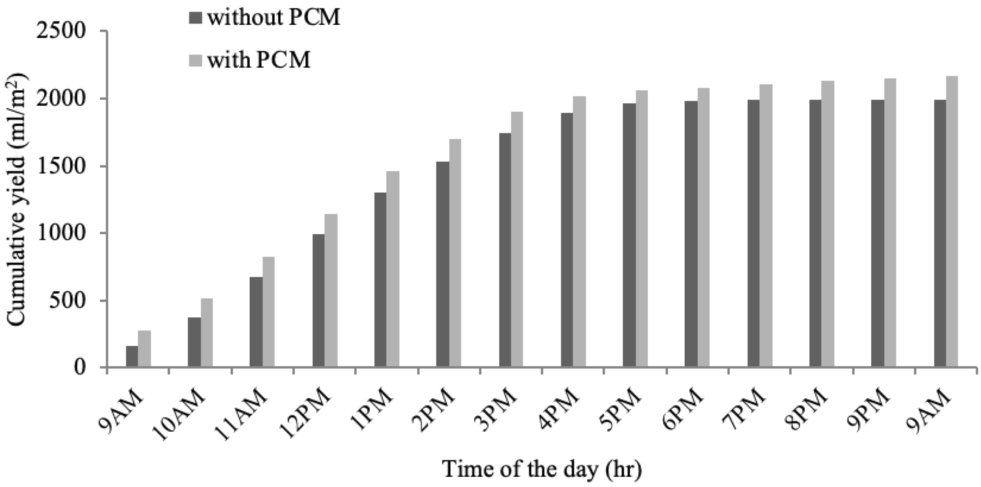

Figure 11. Comparison of the cumulative hourly yield for the still with and without PCM.

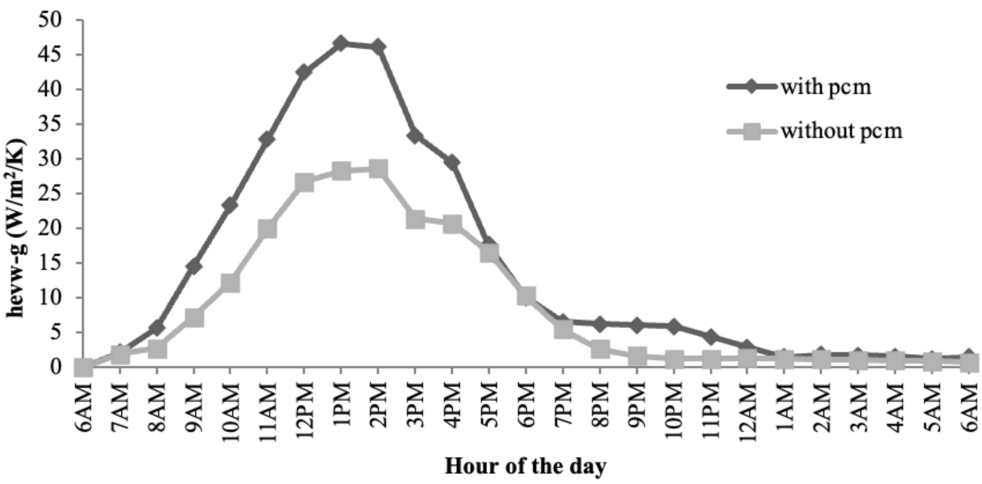

Figure 12. Comparison of the evaporative heat transfer coefficient from water to glass (with and without PCM).

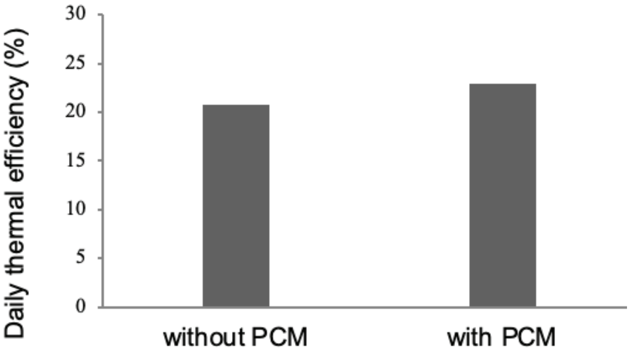

Figure 13. Comparison of the daily thermal efficiencies of the still with and without PCM.

of the still is increased by 10.5% with the incorporation of PCM (Fig. 13). Improvement in the performance of the still with PCM is attributed to the decrease of the total heat losses to the surroundings. Comparison of the hourly variation of the top losses and bottom losses for the still without and with PCM are shown in Figures 14 and 15 respectively. Total heat losses to the surroundings over a day are found to decrease by 7.7% with the incorporation of PCM. From Figure 14 it is observed that the top losses to the surroundings are slightly higher for the still with PCM till 9 AM. During this period, the rate of increase in the temperatures of the components of the still with PCM is higher than that of the still without PCM. Hence the

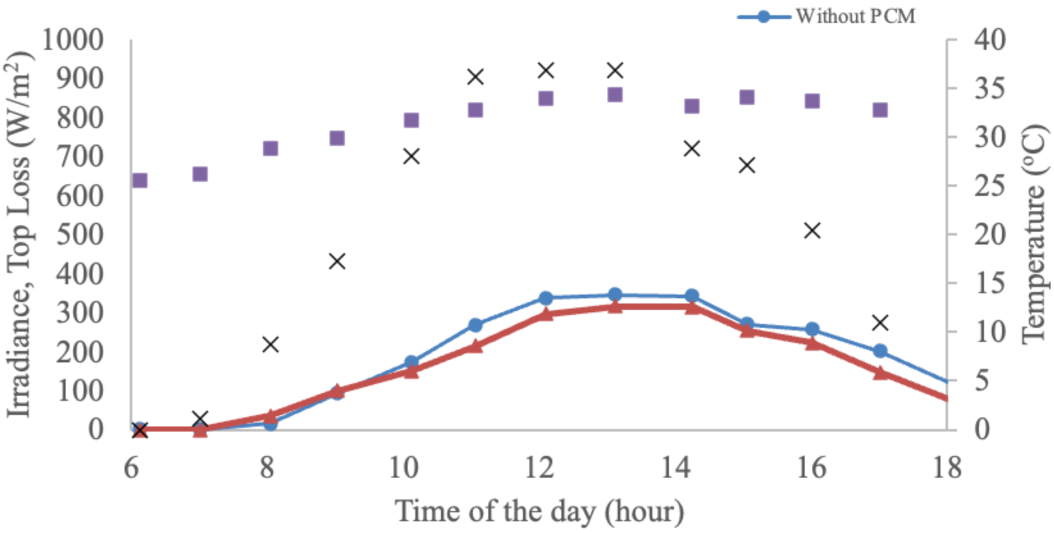

Figure 14. Comparison of top losses for the still without and with PCM.

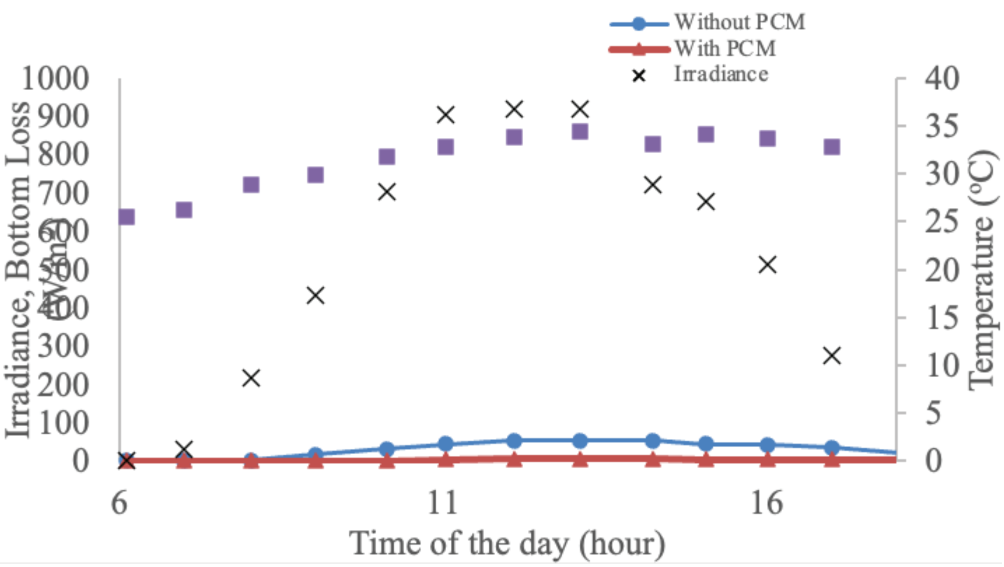

Figure 15. Comparison of bottom losses for the still without and with PCM.

losses are higher for the still with PCM. After 7 PM, heat losses have become almost zero for the still without PCM while the losses prevail till about 7 PM for the still with PCM. However, this is a negligibly small amount. For the still without PCM, the temperatures of all the components of the still have become almost equal to ambient temperature after 7 PM and hence there are no heat losses to the surroundings. In the case of the still with PCM, the water and absorber temperatures are higher than that of ambient temperature as the PCM discharges the heat stored in it to the absorber during this time. Hence, the heat loss to the surroundings is non-zero after 7 PM.

But it may be noted that during sunshine hours, heat losses from the still with PCM are considerably lower than that of the still without PCM. During sunshine hours, PCM stores appreciable amount of incident solar energy which would be lost to the surroundings in its absence. Lauric acid, the PCM used in the present work, has low thermal conductivities of 0.447 W/mK and 0.147 W/mK in the solid and liquid forms respectively. It thus acts as an additional insulating layer thereby reducing the heat losses to the surroundings through the bottom surface of the still. Therefore, the bottom losses are significantly decreased in the case of still with PCM as observed from Figure 15.

The extent of irreversibility in each of the still components is evaluated by evaluating the associated exergy destruction. It is seen from Figures 16 and 17 that in both the cases of the still with and without PCM, maximum exergy destruction is observed in the absorber. Exergy destruction in the water and the glass cover are negligible compared to that of the absorber. The exergy destruction in the absorber for the still with PCM is less compared to the still without PCM. Total exergy destruction in the absorber, saline water and glass cover for the still without PCM are 2089.7 W/m^2, 281.8 W/m^2 and 320.58 W/m^2 respectively over a day. The total exergy destruction over a day in the still without PCM is 2692.08 W/m^2. Total exergy destruction in the absorber, saline water and glass cover for the still with PCM are 1990.9 W/m^2, 280.83 W/m^2 and 341.29 W/m^2 respectively over a day. The total exergy destruction in the still with PCM over a day is 2613.02 W/m^2. Therefore, the exergy destruction is reduced by 3% with the incorporation of PCM. It may be noted that the temperature difference between absorber and water is higher for the still with PCM resulting in higher heat transfer rate from the absorber to water. Therefore, energy that is being utilized for the evaporation of water is more. In other words, the available portion of thermal energy which is being transferred from absorber to the water for its evaporation is more resulting in decreased exergy destruction. Daily exergy efficiency of the still without PCM is 1.66% and with PCM is 1.71%.

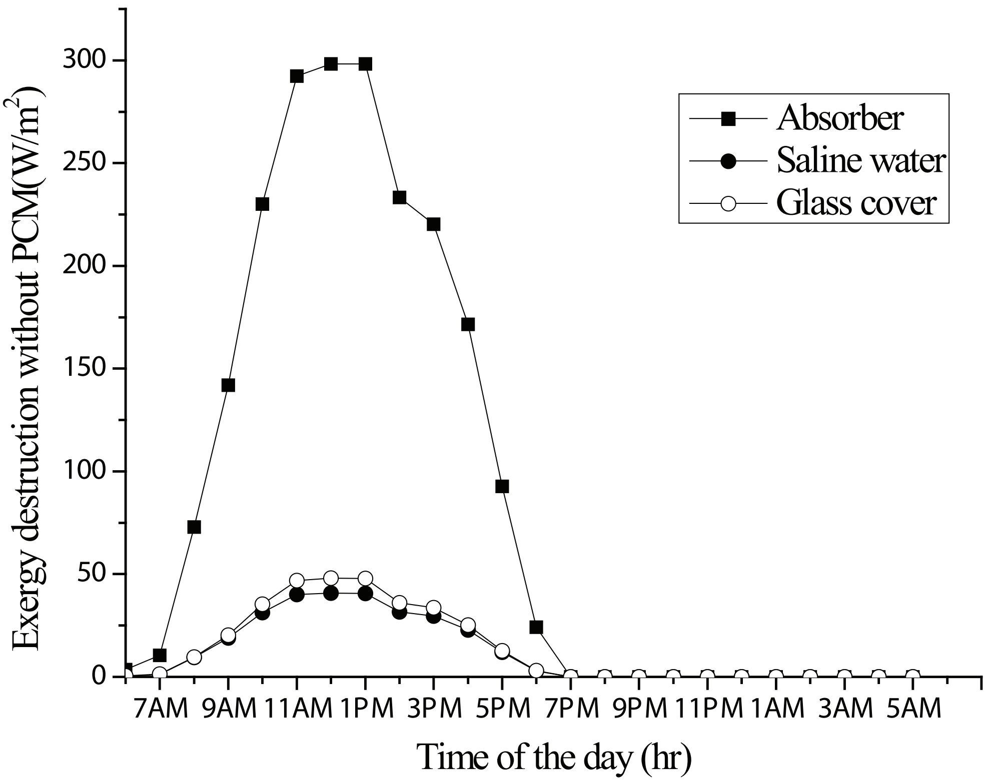

Figure 16. Hourly variation of the exergy destruction in the different parts of the still without PCM.

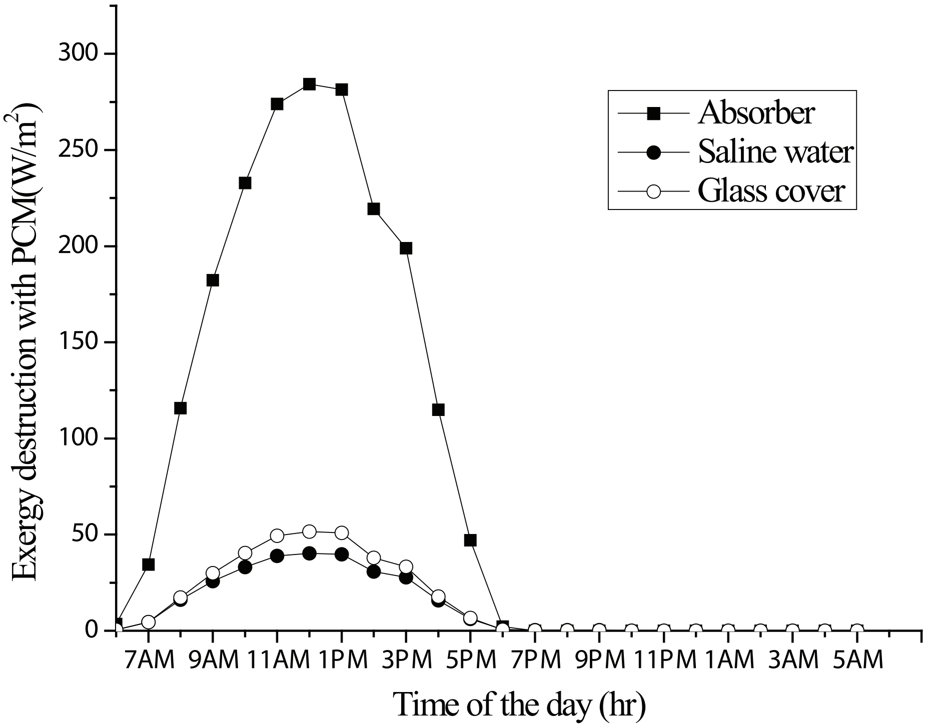

Figure 17. Hourly variation of the exergy destruction in the different parts of the still with PCM.

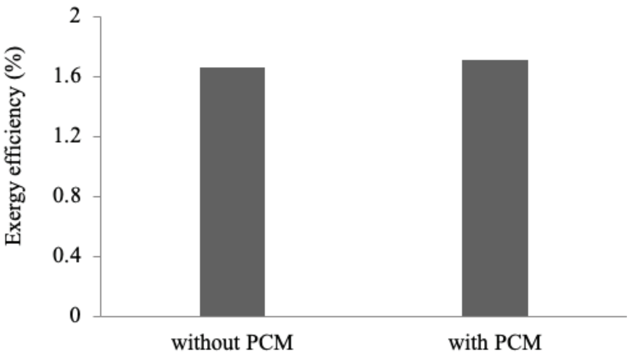

Figure 18. Comparison of the daily exergy efficiencies of the still with and without PCM.

CONCLUSION

Solar still though a simple and passive system, is limited by its low productivity. Incorporation of Phase Change Material enables improvement in its productivity and utilization of the solar energy input in an efficient manner. In the present work, the effect of incorporating lauric acid as the phase change material on the performance of a double slope passive solar still has been investigated for the tropical climate of a south Indian location. Performance assessment of the PCM integrated still was carried out using energy and exergy analysis. System simulation was carried out based on the mathematical model developed and the results obtained were compared with experimental results. From numerical simulations, it was observed that still performance had improved by incorporating PCM based energy storage. Exergy destructions in the components of the still were calculated for both the basic still and for the still integrated with PCM. Maximum exergy destruction was observed in the absorber of the still in both the cases. Exergy destruction in the absorber was reduced by incorporating the PCM. Daily yield, daily thermal and exergy efficiencies were increased by 8.9%, 10.6% and 3% respectively with the incorporation of PCM. A generic modelling framework for energy and exergy-based performance assessment of a PCM integrated still has been presented which will be a useful tool for the system optimization. In the near future, the integration of various PCM with improved thermal characteristics can be investigated together with system optimisation for optimal energy efficiency. Research also needs to concentrate on smart control systems that use AI algorithms for better performance in widely varying weather conditions.

NOMENCLATURE

A	area, m^2
c	specific heat, J/kg K
C	heat capacity, J/K
Ex	exergy rate, W/m^2
h	heat transfer coefficient, $W/m^2 \cdot K$
H	hour

I	solar irradiance, W/m^2
k	thermal conductivity, W/m.K
L	thickness, m
LH	Latent heat of vaporization of water, J/kg
m	mass, kg
M	daily yield, kg/ m^2.day
Nu	Nusselt number
P	vapour pressure, N/m^2
q	heat transfer rate, W
Ra	Rayleigh number
t	time, s
T	temperature, K
U	overall heat transfer coefficient, W/m^{2}K
V	wind speed, m/s

Greek symbols

α	absorptivity
ε	emissivity
δ	increment
ρ	reflectivity
σ	Stefan-Boltzmann constant

Subscripts

a	ambient
b	absorber
c	convection
d	destruction
eff	efficiency
eq	equivalent
e	evaporation
g	glass cover
i	insulation
l	liquid
m	melting
pcm	phase change material
r	radiation
s	solid
S	sun
w	water

AUTHOR CONTRIBUTION

All the authors equally contributed to this work.

DATA AVAILABILITY STATEMENT

The authors confirm that the data that supports the findings of this study are available within the article. Raw data that support the finding of this study are available from the corresponding author, upon reasonable request.

CONFLICT OF INTEREST

The author declared no potential conflicts of interest with respect to the research, authorship, and/or publication of this article.

ETHICS

There are no ethical issues with the publication of this manuscript.

REFERENCES

[1] Agrawal R, Singh KDP. Experimental investigation and computational modelling of double slope solar still integrated with eutectic phase change material. J Energy Storage 2022;52:104802. [CrossRef]

[2] Katekar VP, Deshmukh SS. A review of the use of phase change materials on performance of solar stills. J Energy Storage 2020;30:101398. [CrossRef]

[3] Malaiyappan P, Elumalai N. Review of the productivity of various types of solar stills. Desalin Water Treat 2015;54:3236-3247. [CrossRef]

[4] Thakur VK, Gaur MK, Sagar MK, Tiwari GN. A study on heat and mass transfer analysis of solar distillation system. J Therm Engineer 2021;7:1184-1205. [CrossRef]

[5] Gaur MK, Tiwari GN, Singh P, Kushwah A. Heat transfer analysis of hybrid active solar still with water flowing over glass cover. J Therm Engineer 2021;7:1329-1343. [CrossRef]

[6] Muftah AF, Alghoul MA, Fudholi A, Abdul-Majeed MM, Sopian K. Factors affecting basin type solar still productivity: A detailed review. Renew Sustain Energy Rev 2014;32:430-447. [CrossRef]

[7] Dsilva Winfred Rufuss D, Iniyan S, Suganthi L, Davies PA. Solar stills: A comprehensive review of designs, performance and material advances. Renew Sustain Energy Rev 2016;63:464-496. [CrossRef]

[8] Rani A, Kant R, Suresh S, Kumar A. Experimental investigation on thermal behavior of hybrid single slope solar still. J Therm Engineer 2021;7:677-689. [CrossRef]

[9] Al-Qasaab MR, Abed QA, Abd Al-Wahid WA. Enhancement the solar distiller water by using parabolic dish collector with single slope solar still. J Therm Engineer 2021;7:1001-1015. [CrossRef]

[10] Javadi Yanbolagh D, Saraei, Mazaheri H, Mehrabadi SJ. Exergoeconomic, environmental, economic, and energy-matrices (4E) analysis of three solar distillation systems equipped with condenser and different heaters. J Therm Engineer 2021;7:1640-1653. [CrossRef]

[11] Kalidasa Murugavel K, Sivakumar S, Riaz Ahamed J, Chockalingam KKSK, Srithar K. Single basin double slope solar still with minimum basin depth and energy storing materials. Appl Energy 2010;87:514-523. [CrossRef]

[12] Shanmugan S, Janarthanan B, Chandrasekaran J. Performance of single-slope single-basin solar still with sensible heat storage materials. Desalin Water Treat 2012;41:195-203. [CrossRef]

[13] Nian YL, Huo YK, Cheng WL. Study on annual performance of the solar still using shape-stabilized phase change materials with economic analysis. Sol Energy Mater Sol Cells 2021;230:111263. [CrossRef]

[14] Sharma A, Tyagi VV, Chen CR, Buddhi D. Review on thermal energy storage with phase change materials and applications. Renew Sustain Energy Rev 2009;13:318-345. [CrossRef]

[15] Kabeel AE, Abdelaziz GB, El-Said EMS. Experimental investigation of a solar still with composite material heat storage: Energy, exergy and economic analysis. J Clean Prod 2019;231:21-34. [CrossRef]

[16] Kateshia J, Lakhera V. A comparative study of various fatty acids as phase change material to enhance the freshwater productivity of solar still. J Energy Storage 2022;48:103947. [CrossRef]

[17] Sonker VK, Chakraborty JP, Sarkar A, Singh RK. Solar distillation using three different phase change materials stored in a copper cylinder. Energy Reports 2019;5:1532-1542. [CrossRef]

[18] Cheng WL, Huo YK, Nian YL. Performance of solar still using shape-stabilized PCM: Experimental and theoretical investigation. Desalination 2019;455:89-99. [CrossRef]

[19] Malik MZ, Musharavati F, Khanmohammadi S, Khanmohammadi S, Nguyen DD. Solar still desalination system equipped with paraffin as phase change material: exergoeconomic analysis and multi-objective optimization. Environ Sci Pollut Res 2021;28:220-234. [CrossRef]

[20] Khandagre M, Gupta B, Bhalavi J, Baredar P. Magnesium sulfate heptahydrate as phase change material in double slope solar still. J Therm Engineer 2021;7:196-214. [CrossRef]

[21] Ayoobi A, Ramezanizadeh M. A detailed review investigating the mathematical modeling of solar stills. Front Energy Res 2022;10:1-18. [CrossRef]

[22] El-Sebaii AA, Al-Ghamdi AA, Al-Hazmi FS, Faidah AS. Thermal performance of a single basin solar still with PCM as a storage medium. Appl Energy 2009;86:1187-1195. [CrossRef]

[23] Dashtban M, Tabrizi FF. Thermal analysis of a weir-type cascade solar still integrated with PCM storage. Desalination 2011;279:415-422. [CrossRef]

[24] Ansari O, Asbik M, Bah A, Arbaoui A, Khmou A. Desalination of the brackish water using a passive solar still with a heat energy storage system. Desalination 2013;324:10-20. [CrossRef]

[25] Torchia-Núñez JC, Porta-Gándara MA, Cervantes-de Gortari JG. Exergy analysis of a passive solar still. Renew Energy 2008;33:608-616. [CrossRef]

[26] Asbik M, Ansari O, Bah A, Zari N, Mimet A, El-Ghetany H. Exergy analysis of solar desalination still combined with heat storage system using phase change material (PCM). Desalination 2016;381:26-37. [CrossRef]

[27] Hassan H, Abo-Elfadl S. Effect of the condenser type and the medium of the saline water on the performance of the solar still in hot climate conditions. Desalination 2017;417:60-68. [CrossRef]

[28] Altarawneh I, Rawadieh S, Batiha M, Al-Makhadmeh L, Alrowwad S, Tarawneh M. Experimental and numerical performance analysis and optimization of single slope, double slope and pyramidal shaped solar stills. Desalination 2017;423:124-134. [CrossRef]

[29] Pal P, Yadav P, Dev R, Singh D. Performance analysis of modified basin type double slope multi-wick solar still. Desalination 2017;422:68-82. [CrossRef]

[30] Sarhaddi F, Farshchi Tabrizi F, Aghaei Zoori H, Mousavi SAHS. Comparative study of two weir type cascade solar stills with and without PCM storage using energy and exergy analysis. Energy Conver Manage 2017;133:97-109. [CrossRef]

[31] Ranjan KR, Kaushik SC. Energy, exergy and thermo-economic analysis of solar distillation systems: A review. Renew Sustain Energy Rev 2013;27:709-723. [CrossRef]

[32] Rejeb O, Yousef MS, Ghenai C, Hassan H, Bettayeb M. Investigation of a solar still behaviour using response surface methodology. Case Stud Therm Engineer 2021;24. [CrossRef]

[33] Ben Halima H, Frikha N, Ben Slama R. Numerical investigation of a simple solar still coupled to a compression heat pump. Desalination 2014;337:60-66. [CrossRef]

[34] Boubekri M, Chaker A, Cheknane A. Modeling and simulation of the continuous production of an improved solar still coupled with a photovoltaic/thermal solar water heater system. Desalination 2013;331:6-15. [CrossRef]

[35] Holman JP, Bhattacharya S. Heat Transfer. New York: McGraw-Hill Companies; 2011.

[36] Ranjan KR, Kaushik SC, Panwar NL. Energy and exergy analysis of passive solar distillation systems. Int J Low-Carbon Technol 2016;11:211-221. [CrossRef]

[37] Aghaei Zoori H, Farshchi Tabrizi F, Sarhaddi F, Heshmatnezhad F. Comparison between energy and exergy efficiencies in a weir type cascade solar still. Desalination 2013;325:113-121. [CrossRef]